ARCHIVES OF ACOUSTICS
17, 2, 287–305 (1992)

DISCRETE SOUND INDUCED BY LOW MACH NUMBER FLOW OVER SIDE BRANCH DEEP CAVITY IN A RECTANGULAR DUCT

M. MEISSNER

Institute of Fundamental Technological Research
(00-049 Warszawa, Świętokrzyska 21)

This paper presents a model of the discrete sound induction effect due to a flow over a deep cavity in the wall of a rectangular duct. Theoretical analysis applies shear layer approximation with a vortex sheet, with deflection satisfying the Kutta–Żukowski condition, and an equivalent impedence system of a deep cavity with cavity impedence change in the presence of the flow included. The applied theoretical method makes it possible to determine the effect of resonance modes of the cavity on disturbances of the vortex sheet and also to determine the frequency and relative value of pressure amplitude in the case of a discrete sound.

1. Introduction

The low Mach number flow over a rectangular cavity is accompanied by a characteristic effect of generation of sound with high intensity in narrow frequency bands. The predominant character of narrow band components in the generated sound is reflected in the widely accepted terminology. In accordance with this terminology this type of noise is defined as a sound with discrete frequency or simply, as a discrete sound. In reality the sound spectrum is continuous and besides components with considerable intensity in one or several frequency bands, also a wide-band noise of turbulent origin occurs.

Discrete sound generated by a flow over a rectangular cavity is the effect of an interaction between disturbances of the shear layer and acoustic disturbances induced in a cavity [1, 2]. Several possible variants of flow-acoustic interactions are distinguished in the course of analysis of this effect. In accordance with the classification presented in the paper [3] the relation $l/d > 8$ defines a class of closed cavities where the shear layer adheres to the bottom wall of the cavity (l – dimension of the opening of the cavity in the direction of flow, d – depth of cavity). Open cavities with $l/d < 8$ are the next group. The formation of a shear layer in open cavities proceeds very much like in the case of a free flow. An interaction between the shear layer and trailing edge is an additional source of

flow disturbance [4, 5]. Open cavities are divided into two categories shallow and deep, and the condition $l/d = 1$ sets the boundary between them.

In the case of a deep cavity, for which $l/d < 1$ the effect of discrete sound induction is related with the shear layer instability due to two factors. The influence of resonance modes of the cavity on disturbances of the shear layer is the first factor, while the second one is the flow-acoustic interaction at the leading and trailing edges. If only the first factor occurs in the process of sound generation then the instability of the shear layer can take place solely for frequencies f close to definite values f_m which are determined by the resonance condition for a quarter-wave resonator [6]

$$k\Delta d - \operatorname{ctan}(kd) = 0 \tag{1}$$

and thus

$$f_m \approx \frac{c(2m-1)}{4(d+\Delta d)}, \quad m = 1, 2, 3,... \tag{2}$$

where m defines the acoustic mode; k and c are the wave number and sound velocity, respectively; and Δd is the resonator end correction. In the case in which only the second factor would occur in the process of sound generation, the following relation between the dimension l of the cavity and wave length λ for disturbances of the shear layer [7] is the necessary condition for pulsation induction

$$l/\lambda = n - \gamma, \quad n = 1, 2, 3,... \tag{3}$$

where n defines the hydrodynamic mode, while $2\pi\gamma = \text{const}$ is the phase shift due to the edge effect. Therefore the instability of the shear layer can only occur for strictly defined λ values.

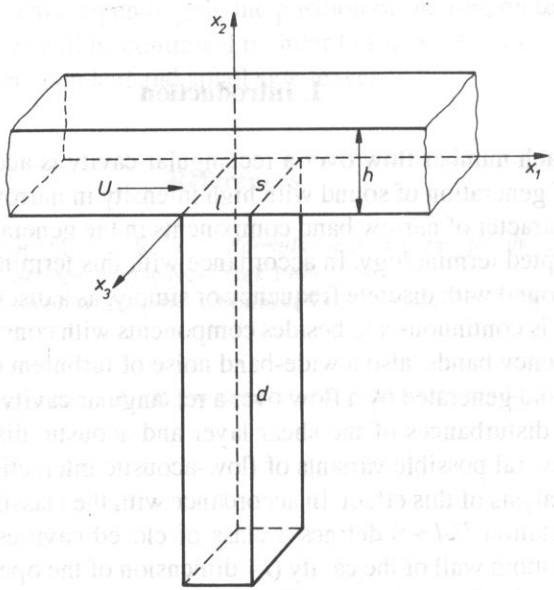

FIG. 1. Deep cavity as a side branch in a rectangular duct l, s – dimensions of cavity, d – depth of cavity, h – hight of duct, U – main flow velocity.

In industrial installations for compressed air transport air discharge channels from the main channel may be a potential source of sound with discrete frequency [8]. Such a situation occurs when the discharge channel is closed while air flows in the main channel. In this paper we analyse the most unfavourable case when the discharge channel joins the main channel under a right angle and forms a deep rectangular cavity during cut-off (Fig. 1). An equivalent impedence system of a deep cavity with a gas stream flowing past it (Subsection 2.1) was used in the presented model and the interaction between resonance modes of the cavity and flow disturbances near the entry to the cavity (Subsection 2.2) was also taken into consideration. Calculation results of dimensionless frequency and values of relative pressure amplitude for discrete sound are compared with the results of measurements presented in paper [8] (Section 3).

2. Theoretical analysis

The case of a flow past a deep cavity with an opening with the following dimensions – l and s (s – perpendicular to the direction of flow) – located in the wall of a rectangular channel is analysed here (Fig. 1). Low Mach number flow in the channel characteristized the main velocity U. Hence, $M^2 << 1$, where $M = U/c$. We assume that the dimension of the opening of the cavity – l and s – and the height of the channel – h – are much smaller than the depth of the cavity – d

$$l/d << 1, \quad s/d << 1, \tag{4}$$

$$h/d << 1 \tag{5}$$

and so for frequencies close to the fundamental frequency f_1 ($m = 1$ in formula (2)) we obtain:

$$kl << 1, \quad ks << 1, \tag{6}$$

$$kh << 1, \tag{7}$$

where $k = 2\pi f/c$. On the basis of the condition (7) we can substitute the shear layer which forms near the opening of the cavity with a vortex sheet. If the displacement of the vortex sheet is defined by the function ξ, which is a harmonic function of t

$$\xi = \xi_a(x_1, x_3)\, e^{-j\omega t}, \tag{8}$$

where $\omega = 2\pi f$ then the velocity components in the direction normal to the plane of the opening just above and just below the vortex sheet are as follows:

$$v(\bar{x}, t)\Big|_{x_2 = +0} = \left(-j\omega + U\frac{\partial}{\partial x_1}\right)\xi = v_+, \tag{9}$$

$$v(\bar{x}, t)\Big|_{x_0 = -0} = -j\omega\xi = v_-, \tag{10}$$

where $\bar{x} = (x_1, x_2, x_3)$. The velocity v is discontinuous for $x_2 = 0$ only when $0 < x_1 < l$, because the velocities v_+ and v_- at the leading edge and the trailing edge must be equal to zero

$$v_{\pm}(x_1 = 0) = v_{\pm}(x_1 = l) = 0. \tag{11}$$

The condition (11) leads to the so-called Kutta–Żukowski boundary condition

$$\xi(x_1 = 0) = \partial\xi/\partial x_1(x_1 = 0) = 0, \tag{12}$$

which says that the vortex sheet can only leave the leading edge tangentially. The condition (12) has another important consequence – the condition of pressure equality on both sides of the vortex sheet is transferred to the leading edge. It would be very difficult to determine the boundary conditions at the trailing edge on the basis of the expression (11). In real conditions the influence of the trailing edge on the disturbances of the shear layer is strongly nonlinear. In order to take this nonlinearity into consideration in the presented linear model, we accepted that the displacement of the vortex sheet undergoes a jump at the trailing edge

$$\begin{aligned} \xi &\neq 0 \quad \text{for } x_1 = l, \\ \xi &= 0 \quad \text{for } x_1 > l. \end{aligned} \tag{13}$$

what means that only the right-hand limit of the function ξ satisfies the boundary condition (11) at the trailing edge. The introduction of nonlinearity of the function ξ at the trailing edge is a necessary condition for flow energy transfer to the cavity and for the induction of self-excited oscillations, as HOWE [9] and KELLER and ESCUDIER [10] papers have proved. This conclusion also finds confirmation in the analysis of an impedance model of a cavity presented in the following part of this paper.

2.1. Impedance model of a deep cavity

It results from the condition (6) that the dimensions of the cavity – l and s – are much smaller than the length of an acoustic wave. Thus the system formed by the deep cavity can be considered as a system with lumped elements. The properties of such a system are characterized by specific acoustic impedance defined as the ratio of acoustic pressure in the plane of the opening of the cavity to the acoustic velocity component in the direction perpendicular to this plane. In the case under analysis, pressure as well as the normal component of velocity depend on the displacement of the vortex sheet and thus are functions of the coordinates x_1 and x_3. Therefore, in an impedance model of a cavity the pressure corresponds with the mean value of pressure on the surface of the opening of the cavity, while the normal component of velocity corresponds with the mean value of the normal component on this surface. In further parts of this paper these quantities will be called mean pressure and mean normal velocity.

As it results from Eqs. (9) and (10), there is a discontinuity of the normal component of velocity in the plane of the opening of the cavity. This leads to a discontinuity of the mean normal velocity. *This means, from the acoustic point of view, that the cavity* treated as a system with lumped elements, can be divided into two systems: outer in which the input signal is determined by the mean normal velocity for $x_2 = +0$, and inner in which the input signal is determined by the mean normal velocity for $x_2 = -0$.

If these quantities are noted as V_1 and V_2, then on the basis of Eqs. (9) and (10) we have

$$V_1 = \frac{1}{ls}\int_0^s\int_0^l \left(-j\omega + U\frac{\partial}{\partial x_1}\right)\xi dx_1 dx_3 = V_2 + \frac{U}{ls}\int_0^s \xi(x_1 = l)\,dx_3 \tag{14}$$

$$V_2 = -\frac{j\omega}{ls}\int_0^s\int_0^l \xi dx_1 dx_3. \tag{15}$$

It results from the conditions of pressure equality on both sides of the vortex sheet that the mean pressure p_s is continuous in the plane of the opening of the cavity. Thus

$$V_1 = -p_s/z_1, \tag{16}$$

$$V_2 = p_s/z_2, \tag{17}$$

where z_1 and z_2 are specific acoustic impedances of the outer and inner system respectively. The minus sign in the expression (16) includes the fact that the phase shift between mean pressure and mean normal velocity is equal to π in the outer system [6]. The formulae (16) and (17) do not characterize the acoustic properties of the whole cavity because they concern the outer and inner system separately. In order to connect these two systems into one and thus obtain an impedance model of the whole cavity, Eqs. (16) and (17) should be substituted in Eq. (14). After conversions we obtain

$$p_s = \frac{z_1 z_2}{z_1 + z_2} V_0, \tag{18}$$

where

$$V_0 = -\frac{U}{ls}\int_0^s \xi(x_1 = l)\,dx_3. \tag{19}$$

Therefore an equivalent impedance system with a parallel connection of impedances of the outer and inner system is the model of the whole cavity. In this model the mean normal velocity V_0 represents the exciting signal and mean pressure p_s is the response to the excitation. As it results from Eq. (18) p_s differs from zero only when $V_0 \neq 0$. Acoustic oscillations can only be induced in the cavity when $\xi(x_1 = l) \neq 0$ (formula (19)) what is equivalent to the assumption that the function ξ which defines the displacement of the vortex sheet is discontinuous on the trailing edge.

2.1.1. Specific acoustic impedance of the outer system

Impedance z_1 of the outer system characterizes the process of acoustic energy exchange between the oscillating medium in the opening of the cavity and the outer medium. When there is no flow the real component of this impedance corresponds with the energy lost in the system (i.e. radiated energy) and the imaginary component corresponds with the energy of the medium oscillating with the system (i.e. energy initially transferred to the medium, but later transferred back to the system due to inertia). In the presence of a flow the energy transfer between the oscillating medium in the opening of

the cavity and the outer medium is much more complex. In real conditions this process determines mutual interactions between acoustic disturbances and the mobile medium. This causes some acoustic energy transfer to the out side [11]. This effect can be included in the analysed flow model which is an idealization of an actual flow, by introducing a modification of impedance z_1. To this end we can take advantage of results of impedance z_1 measurements presented in WALKER's and CHARWAT's paper [12] and the theoretical model suggested by these authors. This model makes it possible to determine changes of impedance z_1 in terms of flow velocity. In accordance with [12], impedance z_1 is the sum of two impedances

$$z_1 = z_1' + z_2'', \tag{20}$$

where z_1' characterizes the process of energy transfer between the oscillating medium in the opening of the cavity and the outer medium with no flow, while z_1' defines the influence of flow on this process

$$z_1'' \approx \frac{\rho c K(M - jkl/2)}{1 + S^2/4}, \tag{21}$$

where K is an empirical constant, $S = \omega l/U$, and ρ is the density of the medium. Impedance z_1 corresponds with the radiation impedance of a rectangular piston with dimensions l and s. Hence, on the basis of [13]

$$z_1' = r_p + j\rho c k \Delta d, \tag{22}$$

$$r_p = \frac{\rho c k^2}{16}\left(l^2 + s^2\right) \tag{23}$$

is the specific acoustic radiation resistance, and

$$\Delta d \approx \frac{8(l^2 + ls + s^2)}{9\pi(l + s)} \tag{24}$$

is the end correction.

2.1.2. Specific acoustic impedance of the inner system

The impedance of the inner system corresponds with the impedance of a rectangular cavity with depth d and other dimensions – l and s, with absorption phenomena included. The effect of acoustic wave damping is related with the occurrence of a tangent force on the walls of the cavity and with losses due to heat exchange between condensations and thinning in the medium. If the depth of the cavity greatly exceeds its other dimensions then the acoustic wave propagating inside the cavity can be considered to be a damped plane wave with a wave-front perpendicular to the axis of the cavity. Thus the velocity potential ϕ in the cavity is as follows

$$\phi_- = \left(A e^{\gamma x_2} + B e^{-\gamma x_2}\right) e^{-j\omega t}, \tag{25}$$

where A and B are constant their ratio depends on the boundary condition on the bottom wall of the cavity ($x_2 = -d$), and $\gamma = \eta + jk$ where η is the attenuation constant [14]

$$\eta = 1.95 \cdot 10^{-5} \left(\frac{\omega}{ls}\right)^{1/2}. \tag{26}$$

The acoustic pressure p and acoustic velocity v in the cavity can be determined on the basis of the expression (25)

$$p = -\rho \frac{\partial \phi_-}{\partial t} = j\rho ck(A e^{\gamma x_2} + B e^{-\gamma x_2}) e^{-j\omega t}, \tag{27}$$

$$v = \frac{\partial \phi_-}{\partial x_2} = \gamma(A e^{\gamma x_2} - B e^{-\gamma x_2}) e^{-j\omega t}. \tag{28}$$

Since $p_s = p(x_2 = 0)$ and $V_2 = v(x_2 = 0)$, then

$$z_2 = p_s / V_2 = \frac{\rho c}{1 - j\eta k} \frac{A/B + 1}{A/B - 1}. \tag{29}$$

If we accept that all walls of the cavity are perfectly rigid then the A/B ratio can be determined by applying the condition $v(x_2 = -d) = 0$ in Eq. (28). We obtain

$$A/B = e^{2\gamma d} \tag{30}$$

and finally

$$z_2 = \frac{\rho c}{1 - j\eta/k} \operatorname{cth}(\gamma d). \tag{31}$$

2.1.3. Average acoustic pressure on the surface of the opening of the cavity

The relationship between the exciting signal represented by the mean normal velocity V_0 and mean pressure p_s – the response of the cavity to the excitation – is determined by the expression (18) in the impedance model of the cavity. In this formula pressure p_s remains unknown. It is equivalent to the mean acoustic pressure p on the surface of the opening of the cavity

$$p_s = \frac{1}{ls} \int_0^s \int_0^l p(x_2 = 0) dx_1 dx_3. \tag{32}$$

Pressure p is continuous for $x_2 = 0$ because p_s can be determined by defining p on the boundary of the outer area, i.e. for $x_2 = +0$. If the function $\phi_+(\bar{x}, t)$ defines the velocity potential for $x_2 > 0$, then the derivative $\partial \phi_+ / \partial x_2$ for $x_2 = +0$ corresponds with the normal component of velocity v_+ (formula (9))

$$v_+(x_1, x_3, t) = \left.\frac{\partial \phi_+}{\partial x_2}\right|_{x_2 = +0}. \tag{33}$$

Applying in Eq. (33) the following identity

$$v_+(x_1, x_3, t) = \int_{-\infty}^{\infty}\int_{-\infty}^{\infty} v_+(y_1, y_3, t)\,\delta(x_1 - y_1)\,\delta(x_3 - y_3)\,dy_1 dy_3 \tag{34}$$

and the formula (9) which defines the dependence of the normal component v_+ on the displacement of the vortex sheet ξ, we obtain

$$\phi_+ = \int_{-\infty}^{\infty}\int_{-\infty}^{\infty}\left[\left(-j\omega + U\frac{\partial}{\partial y_1}\right)\xi_a(y_1, y_3)\right] G(y_2 = 0)\,dy_1 dy_3, \tag{35}$$

where

$$G(\bar{x}, \bar{y}, t), \quad \bar{x} = (x_1, x_2, x_3), \quad \bar{y} = (y_1, y_2, y_3),$$

a Green function which satisfies the following boundary conditions:

$$\frac{\partial G}{\partial x_2}(x_2 = h) = \frac{\partial G}{\partial x_3}(x_3 = 0) = \frac{\partial G}{\partial x_3}(x_3 = s) = 0, \tag{36}$$

$$\frac{\partial G}{\partial x_2}(x_2 = 0) = \delta(x_1 - y_1)\,\delta(x_3 - y_3)\,e^{-j\omega t}, \quad x_1 \in <0, l>, \tag{37}$$

$$\frac{\partial G}{\partial x_2}(x_2 = 0) = 0, \quad x_1 \notin <0, l>. \tag{38}$$

The range of variables y_1 and y_3 in the expression (35) can be limited to intervals: $0 \le y_1 \le l$, $0 \le y_3 \le s$ by extending the conditions $\xi_a(y_1, y_3) = 0$ onto the entire rigid surface limiting the entry to the cavity. This is equivalent to the assumption that the separation of flow only occurs in the entry to the cavity. Since on the boundary of the outer area

$$p(x_2 = 0) = -\rho\left(-j\omega + U\frac{\partial}{\partial x_1}\right)\phi_+(x_2 = 0), \tag{39}$$

then, after substituting Eq. (39) in Eq. (32) and including Eq. (35), we obtain

$$p_s = -\frac{\rho}{ls}\int_0^s\int_0^l\left(-j\omega + U\frac{\partial}{\partial x_1}\right)\int_0^s\int_0^l\left[\left(-j\omega + U\frac{\partial}{\partial y_1}\right)\xi_a(y_1, y_3)\right]\times$$

$$\times\, G(x_2 = 0, y_2 = 0)\,dy_1 dy_3 dx_1 dx_3. \tag{40}$$

Considering Eq. (36) for $x_1 \in <0, l>$, we can present the function G in the following form:

$$G(\bar{x}, \bar{y}, t) = \sum_{n=0}^{\infty}\cos\left(\frac{n\pi x_3}{s}\right)[\,G_n(\bar{x}_0, \bar{y}, t) + G_n(\bar{x}_0, y_1, y_2 = 2h, y_3, t)\,], \tag{41}$$

where $\bar{x}_0 = (x_1, x_2)$. The second expression in square brackets in this formula is an additional component of the Green function. It results from the reflection of the acoustic wave from the top wall of the channel $x_2 = h$. In cases of low Mach number flow and $x_1 \in <0, l>$ the function G_n has the same form as in a case without flow (see the Appendix)

$$G_n = -j\frac{\varepsilon_n \cos(\frac{n\pi y_3}{s})}{2s} H_0^{(1)}[\, k_n\sqrt{(x_1-y_1)^2+(x_2-y_2)^2}\,]\, e^{-j\omega t}, \tag{42}$$

where ε_n is the Neumann constant and $k_n = (k^2 - n^2\pi^2/s^2)^{1/2}$.

2.2. Disturbances of the vortex sheet

It results from Eqs. (19) and (40), that two fundamental parameters in the impedance model of a cavity: mean normal velocity V_0 and mean pressure p_s, depend on the unknown function ξ which defines the displacement of the vortex sheet. In the case under analysis we can accept that sheet disturbances are two-dimensional [15, 16]

$$\xi(x_1, t) = \xi_a(x_1) e^{-j\omega t}, \tag{43}$$

therefore the expression (9) can be noted in the following form:

$$v_+ = (-j\omega + U\frac{\partial}{\partial x_1})\,\xi(x_1, t) \tag{44}$$

As we can see from Eq. (13) the function ξ is discontinuous at the trailing edge ($x_1 = l$). Thus, if $\xi_c(x_1, t)$ denotes the displacement function-continuous on this edge – then on the basis of Eq. (13) we have

$$\xi(x_1, t) = \xi_c(x_1, t)\,[\,1 - H(x_1 - l)\,], \tag{45}$$

where $H(x_1 - 1)$ is the unit step function

$$H(x_1 - l) = \begin{cases} 1, & x_1 > l, \\ 0, & x_1 \le l. \end{cases} \tag{46}$$

Substituting Eq. (45) in Eq. (44) we hence achieve

$$v_+ = (-j\omega\xi_c + U\frac{\partial \xi_c}{\partial x_1})\,[\,1 - H(x_1 - l)\,] - U\,\xi_a(l)\,\delta(x_1 - l)\, e^{-j\omega t}. \tag{47}$$

The introduction of a discontinuity in the function ξ leads to an additional component on the right hand side in Eq. (47). It represents the pulse velocity source. This source is a kind of an external force because, as it was assumed in the theoretical model, the discontinuity function ξ described the nonlinear effects accompanying the interaction between the shear layer and the trailing edge. A vortex sheet influenced by such a source exhibits instability which manifests itself in an amplitude increase of the sheet displacement when the distance from the source grows. If the motion of a vortex sheet located on the boundary of a low Mach number flow with velocity U in an unbounded two-dimensional space (no rigid surfaces) is influenced by a velocity source $-U\,\xi_a(l)\,\delta(x_1 - l)\, e^{-j\omega t}$, then the displacement of an unstable vortex sheet is described with the function ξ_c which is a superposition of Kelvin–Helmholtz waves:

$$\xi_c = M\,\xi_a(l)\left[\, a e^{j\varepsilon(x_1 - l)} + b e^{j\varepsilon^*(x_1 - l)}\right] e^{-j\omega t}, \tag{48}$$

where $\varepsilon = \omega(1 - j)/U$, while ε^* is a quantity conjugate with ε.

In the case if a vortex sheet lies within the area of the opening of the cavity, its unstable motion is a result of the presence of the pulse velocity source at the trailing edge and the influence of an acoustic signal induced in the cavity. Since, in accordance with the condition $kl < 1$, this signal is approximately a plane wave in the plane of the opening of the cavity, we accepted in our approximation method of the function ξ that ξ is a sum of the functions (48) in which an unknown quantity α was introduced in the place of the parameter ε and the component $Qe^{-j\omega t}$, where Q denotes the amplitude of a plane wave acoustic displacement was included. The parameter ε was changed into the parameter α – an unknown function of ω, U, l, s, d, h – in order to include in ξ mutual interactions between disturbances of the vortex sheet and acoustic modes of the cavity. Therefore the following assumption was accepted in the ξ approximation: the acoustic signal induced in the cavity does not change the form of the displacement function in the case of an unstable vortex sheet, it only modifies this function parameters. Hence the form of the function ξ accepted in the theoretical model is as follows:

$$\xi = M\xi_a(l)\left[ae^{j\alpha(x_1-l)} + be^{j\alpha'(x_1-l)}\right]e^{-j\omega t} + Qe^{-j\omega t}, \tag{49}$$

where $\alpha = \alpha_r + j\alpha_i$ and $\alpha_r > 0$, $\alpha_1 < 0$. The displacement of the vortex sheet ξ must satisfy the Kutta–Żukowski condition at the leading edge, thus

$$\xi(x_1, t) = \xi_a(x_1)e^{-j\omega t} = Q\left(1 - \frac{\beta^*}{\beta+\beta^*}e^{\beta x_1/l} - \frac{\beta}{\beta+\beta^*}e^{-\beta^* x_1/l}\right)e^{-j\omega t}, \tag{50}$$

where $\beta = j\alpha l = \beta_r + j\beta_i$ and

$$\beta_r = -\alpha_i l > 0, \quad \beta_i = \alpha_r l > 0. \tag{51}$$

The amplitude Q and parameter β in the formula (50) are unknown quantities. Equation (18) should be used to determine β. This equation defines the relationship between the mean normal velocity V_0 and mean pressure p_s in the impedance model of a cavity. Once we know the form of the function $\xi(x_1, t)$, V_0 can be determined on the basis of Eq. (19)

$$V_0 = \frac{QU}{l}\left(\frac{\beta}{\beta+\beta^*}e^{\beta} + \frac{\beta^*}{\beta+\beta^*}e^{-\beta^*} - 1\right)e^{-j\omega t}, \tag{52}$$

while Eqs. (41) and (42) are included in the expression (40) and is integrated in terms of x_3 and y_3, it can be written in the following form:

$$p_s = \frac{j\rho QU}{2l^2}\int_0^l(-j\omega + U\frac{\partial}{\partial x_1})\int_0^l(\gamma_1 e^{\beta y_1/l} + \gamma_2 e^{-\beta^* y_1/l} - jS)\times$$

$$\times\left\{H_0^{(1)}(k|x_1-y_1|) + H_0^{(1)}\left[k\sqrt{(x_1-y_1)^2+4h^2}\right]\right\}e^{-j\omega t}dy_1dx_1, \tag{53}$$

where $\gamma_1 = \beta^*(jS-\beta)/(\beta+\beta^*)$ and $\gamma_2 = \beta(jS+\beta^*)/(\beta+\beta^*)$. Since $kl << 1$, then the following approximation of the Hankel function [17] can be applied in the formula (53)

$$H_0^{(1)}(k|x_1-y_1|) \approx \frac{2j}{\pi}\ln(k|x_1-y_1|/2), \tag{54}$$

$$H_0^{(1)}\left[k\sqrt{(x_1-y_1)^2+4h^2}\,\right] \approx \sum_{n=0}^{\infty} \varepsilon_n (-1)^n H_{2n}^{(1)}(2kh)\frac{(k|x_1-y_1|/2)^{2n}}{(2n)!} \tag{55}$$

When we substitute Eqs. (52) and (53) in the expression (18) and integrate it in terms of x_1 and y_1 we obtain the following equation

$$\beta = jS + \frac{F_1(\beta)}{F_2(\beta)}. \tag{56}$$

The functions F_1 and F_2 which occur in this expression are:

$$F_1(\beta) = \frac{\pi z_1 z_2}{\rho c M(z_1+z_2)}\left[e^{\beta} - 1 + \frac{\beta}{\beta^*}\left(e^{-\beta^*}-1\right)\right]\beta + \left(\frac{\beta}{\beta^*}\right)^2(\beta^* + jS)\times$$

$$\times\left\{S\left[j\ln(kl/2) - \frac{\pi}{2}\right](e^{-\beta^*}-1) + \frac{1}{2}\pi S\Sigma_1 + (\beta^*+jS)\left[\Sigma_3(-\beta^*) + \frac{1}{2}j\pi\Sigma_4(-\beta^*)\right]\right\} +$$

$$+ S^2\left[\frac{3}{2} - \ln(kl/2) + j\pi\sigma_2\right]\left(1+\frac{\beta}{\beta^*}\right)\beta, \tag{57}$$

$$F_2(\beta) = S[\,j\ln(kl/2) - \frac{\pi}{2}\,](1-e^{\beta}) - \frac{1}{2}\pi S\Sigma_1 + (\beta - jS)\,[\,\Sigma_3(\beta) + \frac{1}{2}j\pi\Sigma_4(\beta)\,] \tag{58}$$

where Σ_1, Σ_2, Σ_3 and Σ_4 are series as follows:

$$\Sigma_1 = \sum_{n=0}^{\infty} \frac{\varepsilon_n(-1)^n(kl/2)^{2n}H_{2n}^{(1)}(2kh)}{(2n+1)!}, \tag{59}$$

$$\Sigma_2 = \sum_{n=0}^{\infty} \frac{\varepsilon_n(-1)^n(kl/2)^{2n}H_{2n}^{(1)}(2kh)}{(2n+2)!}, \tag{60}$$

$$\Sigma_3(z) = \sum_{n=1}^{\infty} \frac{1+(-1)^n e^z}{n\cdot n!} z^{n-1}, \tag{61}$$

$$\Sigma_4(z) = 2\sum_{n=1}^{\infty}(-1)^n(kl/2)^{2n}H_{2n}^{(1)}(2kh)\sum_{m=0}^{2n-1}\frac{1+(-1)^m e^z}{(2n-m)!}z^{-m-1}. \tag{62}$$

In the case of the accepted particular geometry of the system (h, l, s and d are given) Eq. (56) can be presented in the following form

$$\beta_r + j\beta_i = F(f, U, \beta_r, \beta_1), \tag{63}$$

where F is the function found on the right hand side in Eq. (56). Thus we have

$$\beta_r = \mathrm{Re}\,[F(f, U, \beta_r, \beta_i)], \tag{64}$$

$$\beta_i = \mathrm{Im}\,[F(f, U, \beta_r, \beta_i)]. \tag{65}$$

Since the frequency f and velocity U are independent variables then for f = const and U = const Eqs. (64) and (65) represent a set of equations with two unknown quantities –

β_r and β_i. A numerical procedure is necessary to solve these equations. Roots sought for are such values of β_r and β_i which satisfy the conditions (51).

2.3. *Discrete sound frequency*

The cavity in experimental studies presented in the paper [8] had the same square section as the main channel, $h = l = s = 6$ cm and depth $d = 53$ cm. The frequency f_d of the discrete sound was determined on the basis of changes of pressure amplitude p_0 measured at the bottom wall of the cavity in terms of f.

If we accept $x_2 = -d$, the pressure p_0 can be determined from the expression (27). Hence we have

$$p_0 = j\rho ck(Ae^{-\gamma d} + Be^{\gamma d})e^{-j\omega t}, \tag{66}$$

where $A = Be^{2\gamma d}$ on the basis of Eq. (30). The relationship between p_0 and p_s can be determined on the basis of the fact that p_s – the pressure in the plane of the opening of the cavity–corresponds with the p value from the expression

$$p_0 = Pe^{j\varphi} = \frac{p_s}{\mathrm{ch}(\gamma d)}, \tag{67}$$

where $P = |p_0|$ and φ is the amplitude and phase of pressure p_0, respectively. Substituting Eq. (18) and including Eq. (52) in Eq. (67), we obtain

$$P = Q\left[\frac{U}{l}\left|\frac{z_1 z_2}{(z_1 + z_1)\mathrm{ch}(\gamma d)}\left(\frac{\beta}{\beta + \beta^*}e^{\beta} + \frac{\beta^*}{\beta + \beta^*}e^{-\beta^*} - 1\right)\right|\right]. \tag{68}$$

Since the parameter $\beta = \beta_r + j\beta_i$ is a function of f and U then for fixed values h, l, s and d Eq. (68) can be presented in the following form:

$$P(f, U) = Q \cdot g[f, U, \beta_r(f, U), \beta_i(f, U)], \tag{69}$$

where g is the function to be found in square brackets on the right hand side in Eq. (68). For frequency $f = f_d$ amplitude P achieves a maximum in terms of f, so

$$P_d(U) = P(f_d, U) = \{Q \cdot g[f, U, \beta_r(f, U), \beta_i(f, U)]\}_{\max}. \tag{70}$$

The results of calculations of the parameters β_r and β_i (roots of the set of Eqs. (64) and (65)), presented in Fig. 2, illustrate a typical dependence of these quantities on the frequency f for $U = \mathrm{const}$ in the case of a cavity with the following dimensions: $h = l = s = 6$ cm and $d = 53$ cm. We can see that the function $\beta_r(f)$ achieves a distinct maximum for a certain frequency f (Fig. 2a). Also the greatest changes in the parameter β_i are observed around this frequency (Fig. 2b). Relative changes of the function g for quantities β_r and β_i determined from Figs. 2a, b are of similar character as changes of β_r in terms of f (Fig. 2c). This indicates that the values of the function g depend on the real part of β mainly.

As we can see from Fig. 2c, the function g reaches a maximum in a very narrow frequency f range. This makes this function similar to spectral characteristics typical for

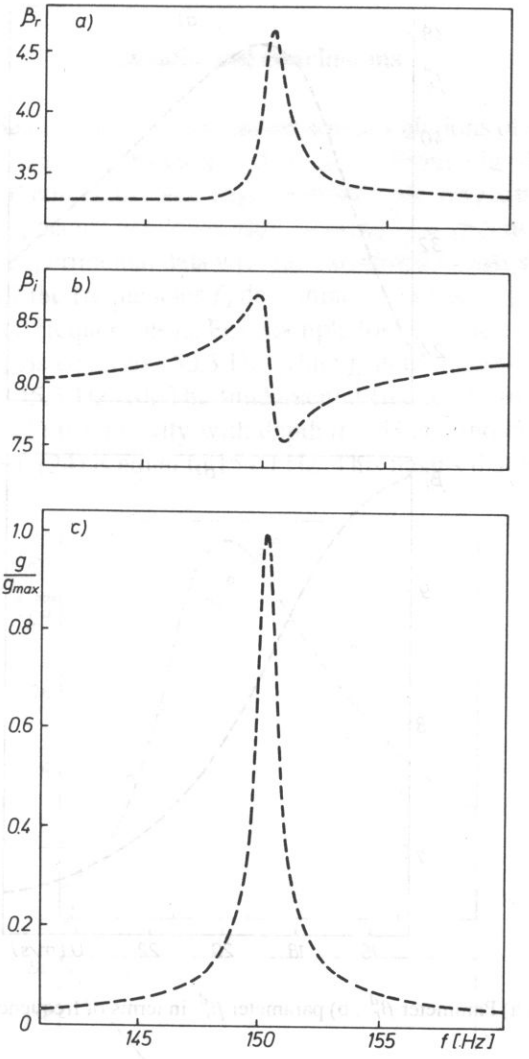

FIG. 2. a) Parameter β_r, b) parameter β_i, c) relative value of function g from the expression (69) in terms of frequency f. Flow velocity $U = 19.5$ m/s.

discrete sound. Therefore basing on the assumption that the parameter Q influences the function P in terms of f only slightly, and here

$$P_d(U) = Q \cdot g\,[f_d, U, \beta_r^d(U), \beta_i^d(U)\,], \tag{71}$$

where $\beta_r^d(U) = \beta_r(f_d, U)$, $\beta_i^d(U) = \beta_i(f_d, U)$. Figure 3 presents calculation results of the parameters β_r^d and β_i^d for a range of flow velocity from 15 to 26 m/s. We can observe that changes of β_r^d and β_i^d which accompany an increase of U are clearly of a

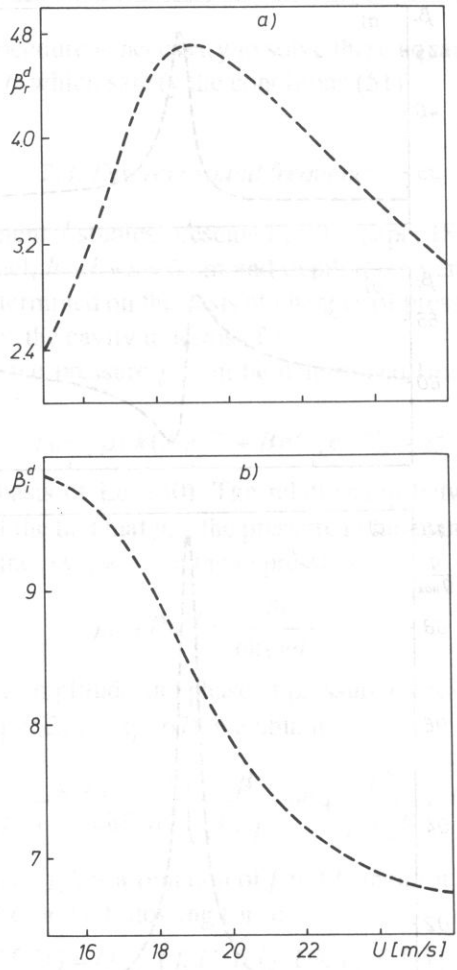

FIG. 3. a) Parameter β_r^d, b) parameter β_i^d in terms of frequency velocity U.

different character. The function which describes β_r^d in terms of U has a maximum (Fig. 3a) while the value of β_i^d always decreases when U grows (Fig. 3b). Since the value of the function g depends mainly on the parameter β_r^d the function $g[f_d, U, \beta_r^d(U), \beta_i^d(U)]$ reaches a maximum within the flow range 15–26 m/s, as it results from Fig. 3. If we make a hypothesis that the parameter Q also only insignificantly influences the function P_d in terms of U, then relative changes of P_d will correspond with relative changes of the function g. Hence

$$\frac{P_d(U)}{[P_d(U)]_{\max}} = \frac{g[f_d, U, \beta_r^d(U), \beta_i^d(U)]}{\{g[f_d, U, \beta_r^d(U), \beta_i^d(U)]\}_{\max}}. \tag{72}$$

3. Results and conclusions

Figure 4 presents the results of measurements and calculations of the $P_d/(P_d)_{\max}$ ratio as well as of the dimensionless frequency $St = f_d l/U$. From Fig. 4a we can see that $P_d/(P_d)_{\max}$ determined theoretically and experimentally are very similar, but the maximum value of $P_d/(P_d)_{\max}$ occurs at a lower flow velocity $U = 19.5$ m/s.

When we compare experimental data with the calculated results shown in Fig. 4b we notice that the values of the frequencies f_d determined theoretically are always slightly higher than the measured frequencies f_d. For example for $P_d/(P_d)_{\max} = 1$ the theoretically determined frequency f_d is equal to 150.3 Hz, while f_d determined from experiment for $P_d/(P_d)_{\max}$ is equal to 145.5 Hz [8]. The fundamental frequently frequency f_1 is calculated from the formula (2) for a cavity with depth $d = 53$ cm and end correction determined on the basis of Eq. (24) is equal to 154.4 Hz. This means that the maximum gene-

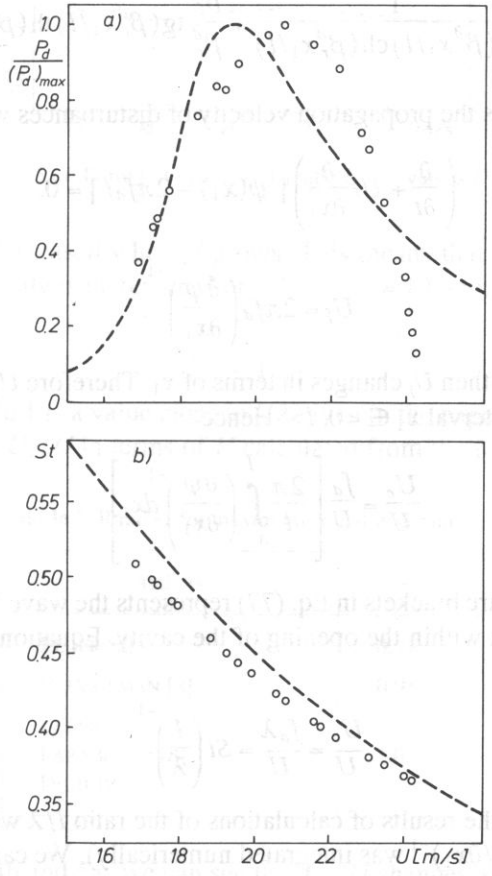

FIG. 4. a) Ratio $P_d/(P_d)_{\max}$, b) dimensions frequency St in terms of velocity(---) – calculated values, (...) – measurement results in accordance with [8].

ration of discrete sound occurs at a frequency f_d slightly lower than the fundamental frequency f_1 of the cavity.

The ratio of propagation velocity U_c of flow disturbances within the opening of the cavity and main flow velocity U is a quantity frequently determined theoretically and experimentally. The velocity U_c presented in the theoretically model in Section 2 is equivalent to the mean phase velocity U_f for disturbances of the vortex sheet described with the function (50) for $f = f_d$. In order to determine U_f, Eq. (50) must be converted into the following form

$$\xi(x_1, t) = |\xi_a(x_1)|\, e^{j[\psi(x_1) - 2\pi f_d t]}, \tag{73}$$

where

$$\psi(x_1) = \operatorname{arctg}\left\{\left[\operatorname{tg}(\beta_i^d x_1/l) - \frac{\beta_i^d}{\beta_r^d}\operatorname{th}(\beta_r^d x_1/l)\right]\times\right.$$

$$\left.\times\left[1 - \frac{1}{\cos(\beta_i^d x_1/l)\operatorname{ch}(\beta_r^d x_1/l)} + \frac{\beta_i^d}{\beta_r^d}\operatorname{tg}(\beta_i^d x_1/l)\operatorname{th}(\beta_r^d x_1/l)\right]^{-1}\right\}. \tag{74}$$

The velocity U_f defines the propagation velocity of disturbances with constant phase

$$\left(\frac{\partial}{\partial t} + U_f\frac{\partial}{\partial x_1}\right)[\,\psi(x_1) - 2\pi f_d t\,] = 0, \tag{75}$$

and thus

$$U_f = 2\pi f_d\left(\frac{\partial\psi}{\partial x_1}\right)^{-1}. \tag{76}$$

Since $\partial\psi/\partial x_1 \neq \text{const}$, then U_f changes in terms of x_1. Therefore U_c corresponds with the mean value U_f in an interval $x_1 \in \langle 0, l\rangle$. Hence

$$\frac{U_c}{U} = \frac{f_d}{U}\left[\frac{2\pi}{l}\int_0^l\left(\frac{\partial\psi}{\partial x_1}\right)^{-1}dx_1\right]. \tag{77}$$

The expression in square brackets in Eq. (77) represents the wave length λ for disturbances of the vortex sheet within the opening of the cavity. Equation (77) can be the noted as follows:

$$\frac{U_c}{U} = \frac{f_d\lambda}{U} = St\left(\frac{l}{\lambda}\right)^{-1}. \tag{78}$$

Figure 5 presents the results of calculations of the ratio l/λ within the flow velocity range 15–26 m/s ($(\partial\psi/\partial x_1)^{-1}$ was integrated numerically). We can see from Fig. 5a that the ratio l/λ changes within the limits

$$0.86 \leq 1\ /\lambda \leq 1.33, \tag{79}$$

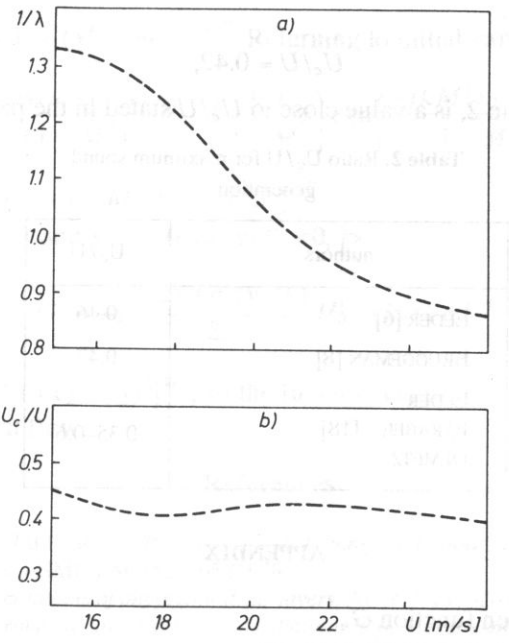

FIG. 5. a) Ratio l/λ versus U, b) ratio U_c/U versus U.

and its value always decreased when U grows. This means that the wave length λ increases when flow velocity is increased. For velocity $U = 19.5$ m/s, when $P_d/(P_d)_{\max}$

$$l/\lambda = 1.1, \tag{80}$$

what according to Table 1 is a value close to l/λ given in the papers [8], [18].

Figure 5b presents U_c/U in terms of U calculated from the formula (78) for values

Table 1. Ratio l/λ for maximum sound generation

authors	l/λ
ELDER [6]	0.77
BRUGGEMAN [8]	0.91
ELDER FARABEE [18] DEMETZ	1.05

St and l/λ from Figs. 4b and 5a. We can see that U_c/U changes are insignificant within the flow velocity range 15–26 m/s because

$$0.4 \leq U_c/U \leq 0.45. \tag{81}$$

when $P_d/P_{d\max} = 1$

$$U_c/U = 0.42, \tag{82}$$

what, according to Table 2, is a value close to U_c/U stated in the papers [6], [8].

Table 2. Ratio U_c/U for maximum sound generation

authors	U_c/U
ELDER [6]	0.46
BRUGGEMAN [8]	0.47
ELDER FARABEE [18] DEMETZ	0.35–0.6

APPENDIX

Calculation of Green function G_n.

The function G_n is a solution of the equation

$$\sum_0^\infty \cos(n\pi x_3/s)\left(\nabla^2 G_n - 2jkM\frac{\partial G_n}{\partial x_1} - M^2\frac{\partial^2 G_n}{\partial x_1^2} + k_n^2 G_n\right) = \delta(\bar{x}-\bar{y})\,e^{-j\omega t}, \tag{A1}$$

where $k_n = (k^2 - n^2\pi^2/s^2)^{1/2}$. After multiplying A1 by $\cos(n\pi x_3/s)$ and integrating it with respect to x_3 within the interval $x_3 \in <0, s>$, we obtain

$$\nabla^2 G_n - 2jkM\frac{\partial G_n}{\partial x_1} - M^2\frac{\partial^2 G_n}{\partial x_1^2} + k_n^2 G_n =$$

$$= \frac{\varepsilon_n \cos(n\pi y_3/s)}{s}\,\delta(x_1-y_1)\,\delta(x_2-y_2)\,e^{-j\omega t}. \tag{A2}$$

When we apply the following conversion of variables in Eq. (A2)

$$x_1' = \mu^2 x_1,\ y_1' = \mu^2 y_1',\ x_2' = \mu x_2,\ y_2' = \mu y_2,\ t' = t + \mu^2 M(x_1 - y_1)/c, \tag{A3}$$

where $\mu = (1-M^2)^{-\frac{1}{2}}$, we have

$$\nabla^2 G_n + k_n^2 G_n = f(y_3)\,\delta(x'_1 - y'_1)\,\delta(x'_2 - y'_2)\,e^{-j\omega t'}, \tag{A4}$$

where $f(y_3) = \mu^2\dfrac{\varepsilon_n \cos(n\pi y_3/s)}{s}$. Equation (A4) is a inhomogeneous wave equation in two-dimensional space, therefore, when we include the condition (38) we have

$$G_n = -\frac{1}{2}jf(y_3)H_0^{(1)}(k_n r')\,e^{-j\omega t'}, \tag{A5}$$

where $r' = [\,(x_1' - y_1')^2 + (x_2' - y_2')^2\,]^{1/2}$. Returning to initial variables we obtain

$$G_n = -j\frac{\varepsilon_n \cos(n\pi y_3/s)}{2s(1-M^2)} H_0^{(1)}\left(\frac{k_n r}{1-M^2}\right)\exp\left(\frac{-jkM(x_1-y_1)}{1-M^2} - j\omega t\right), \tag{A6}$$

where $r' = [\,(x_1 - y_1)^2 + (1-M^2)(x_2 - y_2)^2\,]^{1/2}$.
When $M^2 << 1$, $kl << 1$ and $x_1 \in <0, l>$, $y_1 \in <0, l>$

$$G_n \approx -j\frac{\varepsilon_n \cos(n\pi y_3/s)}{2s} H_0^{(1)}(k_n r)\, e^{-j\omega t}, \tag{A7}$$

where $r = [(x_1 - y_1)^2 + (x_2 - y_2)^2]^{1/2}$, so the function G_n has the same form as it would have in a case without flow.

References

[1] D. ROCKWELL, E. NAUDASCHER, *Review – self-sustaining oscillations of flow past cavities*, J. Fluids Engineering, Trans. ASME **100**, 152–165 (1978).

[2] D. ROCKWELL, *Oscillations of impinging shear layers*, AIAA J. **21**, 5, 645–664 (1983).

[3] V. SAROHIA, *Experimental investigation of oscillations in flow over shallow cavities*, AIAA J. **15**, 7, 984–991 (1977).

[4] A.J. BILANIN, E.E. COVERT, *Estimation of possible excitation frequencies for shallow rectangular cavities*, AIAA J. **11**, 3, 347–351 (1973).

[5] C.K. TAM, P.J. BLOCK, *On the tones and pressure oscillations induced by flow over rectangular cavities*, J. Fluid Mech. **89**, 373–399 (1978).

[6] S.A. ELDER, *Self-excited depth-mode resonance for wall-mounted cavity in turbulent flow*, J. Acoust. Soc. Am. **64**, 3, 877–890 (1978).

[7] J.E. ROSSITER, *Wind tunnel experiments on the flow over rectangular cavities at subsonic and transonic speeds*, RAE Report No. 64037, (1964).

[8] J.C. BRUGGEMAN, *Flow induced pulsations in pipe systems*, Ph.D. thesis, Eindhoven, 1987.

[9] M.S. HOWE, *The influence of mean shear on unsteady aperture flow, with application to acoustical diffraction and self-sustained oscillations*, J. Fluid Mech. **109**, 125–146 (1981).

[10] J.J. KELLER, M.P. ESCUDIER, *Flow-excited resonances in covered cavities*, J. Sound Vib. **86**, 2, 199–226 (1983).

[11] P.A. NELSON, N.A. HALLIWELL, P.E. DOAK, *Fluid dynamics of a flow excited resonance, part II: flow acoustic interaction*, J. Sound Vib. **91**, 3, 375–402 (1983).

[12] B.E. WALKER, A.F. CHARWAT, *Correlation of the effects of grazing flow on impedance of Helmholtz resonators*, J. Acoust. Soc. Am. **72**, 2, 550–555 (1982).

[13] P.M. MORSE, K.U. INGARD, *Theoretical acoustics*, McGraw-Hill, New York 1968, p. 394.

[14] L.E. KINSLER, A.R. FREY, *Fundamentals of acoustics*, John Wiley, New York 1962, p. 241.

[15] L.F. EAST, *Aerodynamically induced resonance in rectangular cavities*, J. Sound Vib. **3**, 3, 277–287 (1966).

[16] E.E. COVERT, *An approximate calculation of the onset velocity of cavity oscillations*, AIIA J., **8**, 12, 2189–2194 (1970).

[17] N.N. LEBEDIEW, *Special functions and their applications* (in Polish), PWN, Warszawa 1957, pp. 135, 146.

[18] S.A. ELDER, T.M. FARABEE, F.C. DEMETZ, *Mechanisms of flow-excited tones at low Mach number*, J. Acoust. Soc. Am., **72**, 2, 532–549 (1982).

Received November 15, 1989, English version October 15, 1991